

Contactless Finger Knuckle Authentication under Severe Pose Deformations

Ajay Kumar

Department of Computing, The Hong Kong Polytechnic University
Hung Hom, Kowloon, Hong Kong
Email: ajaykr@ieee.org

Abstract—Contactless biometrics identification using finger knuckle images has shown significant potential for the e-business and forensic applications. One of the key challenges in accurately matching the real-world contactless finger knuckle images is related to the knuckle pattern deformations that are involuntarily generated due to finger pose changes. Earlier work in this area therefore acquired fixed pose finger images for the authentication and therefore the performance achieved from such images cannot reflect the expected performance under the deployment scenarios. This paper adopts a new approach to accurately match such finger knuckle images and presents first attempt to authenticate finger-knuckle patterns under severe pose changes. This approach attempts to correct pose related deformations by identifying the correspondence between a fixed number of chosen points between two matched images. The match score is computed using local feature descriptors, at each of these correspondence points, and consolidated to generate average match score. The experimental results are presented in this paper, both using two-session and single-session index finger knuckle images from 221 different subjects, using publicly available database. These results are outperforming and indicate the merit of spatial-domain approach to match deformed finger knuckle images using a fixed number of correspondence points.

Keywords— *Biometrics, Forensics, Contactless Finger Knuckle, Pose Invariant Finger Authentication*

I. INTRODUCTION

Personal identification using anatomical characteristics from human body have attracted a number of researchers and system integrators in developing a range of civilian and law-enforcement applications. Several physiological and behavioral features have been studied in the biometrics literature to evaluate their effectiveness for the real-world e-security and forensic applications. Despite increasing applications in forensics and law-enforcement applications, contactless finger knuckle is one of the least studied biometric trait and technologies to utilize its full potential are yet to be developed. High agility of finger knuckle joints, *i.e.* proximal interphalangeal (PIP) joint, can result in severe deformations

on the knuckle surface. Therefore, earlier research work in the literature [4]-[8] employed finger knuckle images acquired with a *fixed* pose where the middle phalanx and proximal phalanx appear along a straight line. A range of spectral and spatial domain methods have been introduced to match finger knuckle images. The accuracy of matching such images depends on the acquisition mode and fixed pose images acquired from a fixed device have shown to offer very high accuracy, *e.g.* [5]. Further efforts to use images acquired from over 500 different subjects with the mobile camera, under ambient illumination, have shown degradation in match accuracy [8] but represents an important step towards developing highly accurate matching capability for the ubiquitous knuckle identification using mobile devices.

II. MOTIVATION AND CHALLENGE

Contactless finger knuckle matching has attracted increasing attention in the literature [4] and a range of databases are available in the public domain. All prior databases (see summary in [4]) were acquired with high degree of user cooperation where the subjects are expected to present their fingers with straight pose, *i.e.* in a manner that allows rich information from the major finger knuckle to be aggregated from the additional skin which is anatomically present to enable the finger movements in the forward direction. Recently [2] released a completely contactless finger knuckle database which presents finger knuckle images with varying poses. Such images are more realistic to develop advanced or ubiquitous biometrics identification capabilities for a range of civilian and law-enforcement applications. This is however a challenging task as the matching accuracy significantly degrades when images with different poses are matched. In addition, the results in [2] were *only* presented for the recognition and no attempt was made to study the authentication performance.

This paper presents a new approach for more accurate contactless finger knuckle authentication under severe finger pose changes. It is first attempt to match completely contactless finger knuckle images with varying poses for the



Figure 1: Sample images from index finger major knuckle with deformations caused by the variation in finger poses. Knuckle creases in red colour are *manually* added to illustrate such variations in the corresponding knuckle creases when the angle between *phalanges* is varied from zero degrees towards extreme (left to right). These images of major knuckle patterns are from the same finger. Therefore, such images should be accurately matched among themselves to realize completely contactless and pose-invariant finger knuckle authentication.

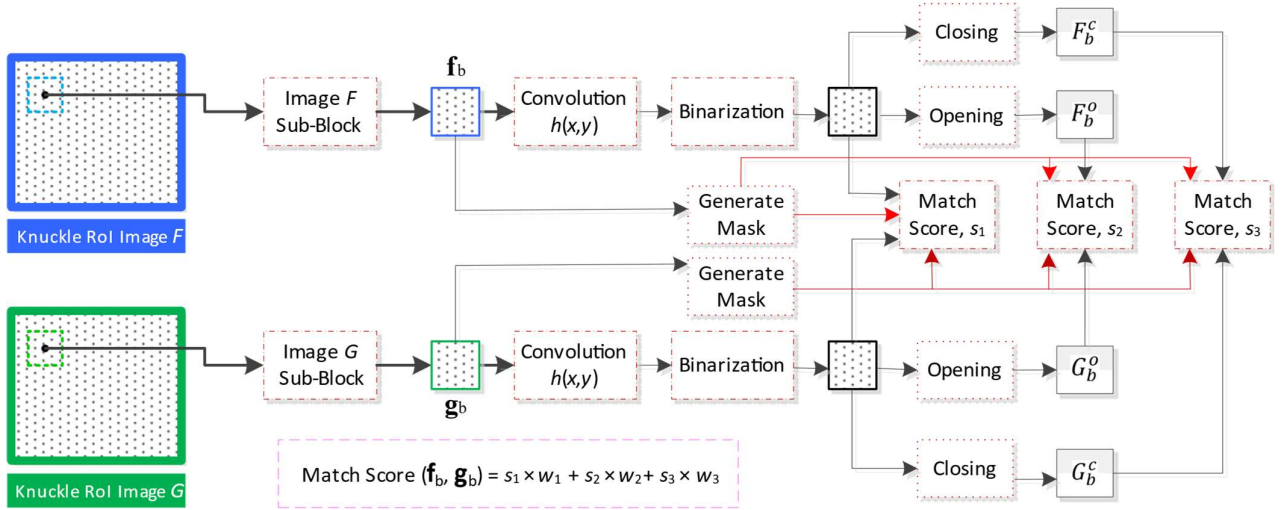


Figure 2: Block diagram to match two key point regions between knuckle image pairs for the user authentication.

user authentication. It should be noted that the finger knuckle images considered in this research have very high intra-class variations due to pose changes and are most challenging as compared to the other publicly available finger knuckle databases. Figure 1 presents such sample images from the one subject in this database. The method introduced in [2] presented encouraging results for the recognition performance but this approach is not suitable to achieve high match accuracy for the verification problem. Therefore we introduce a new approach to match such deformed finger knuckle images. The experimental results presented in this paper indicate outperforming results, both for the single session and two session matching, and validates the effectiveness of this approach for the finger knuckle authentication.

III. FINGER KNUCKLE ALIGNMENT AND MATCHING

The algorithm adopted in this work to match contactless finger knuckle images is similar to the one introduced in [12] to match contactless palmprint images. This work is motivated by the success of local feature descriptors in [8]-[9] and the spectral domain approach to align two region of interest images using [1], [3]. Unlike earlier attempts [23] which used finger knuckle images acquired using contact-based and constrained imaging setups, this work is focused on matching completely contactless finger knuckle images with severe pose deformations.

Each of the two-finger knuckle region of interest (RoI) images, say G and F , are firstly marked with equally spaced $n \times n$ grid points which serve as the reference points align the local regions in two images. Each of the knuckle RoI images are normalized to 128×128 pixels and 13×13 grid points are marked with the spacing of 6 pixels between the neighboring points. The important task is to locate correspondence points in two deformed images. The method detailed in [1] attempts to compute the correspondence, *i.e.*, extent of horizontal and vertical displacements for two grid-points, between two sub-image regions using phase only correlation function. This approach has shown to offer accurate estimation of required displacements for the palmprint [3] and finger knuckle [23] images. Therefore, this approach was incorporated in this work with some modifications. The block diagram for various steps in matching, each of the corresponding image sub-blocks say \mathbf{f}_b and \mathbf{g}_b , for every key point is shown in Figure 2.

More details on the exact steps to extract correspondence points between two images are provided in [1], [23]. The match score between the local regions representing the correspondence points is computed using their local feature descriptors [8]-[9]. A spatial filter with integer values, 1 or -1, is employed to perform local convolution with every pixels in the local regions corresponding to the correspondence points. Among various possibilities, one such spatial filter $h(x, y)$ to encode the ordinal measurements can be defined as follows:

$$h(x, y) = \begin{cases} 1 & \text{if } |x| < |y| \\ -1 & \text{if } |x| > |y| \\ 0 & \text{if } |x| = |y| \end{cases} \quad (1)$$

The variables x, y represents spatial locations in the filter while the $|\cdot|$ is the absolute operation. This spatial filter can be visualized as in the following or Figure 3(a) where above three values are shown with light gray, dark gray and white pixels.

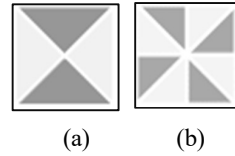


Figure 3: Spatial filter (a)-(b) to encode local feature descriptors.

Similar to as in [12], the binarized features for each of the (sub) image block corresponding to the correspondence points is computed as follows:

$$F_b(x, y) = \begin{cases} 1 & \text{if } f_b(x, y) * h(x, y) > 0 \\ 0 & \text{otherwise} \end{cases} \quad (2)$$

where $*$ represents pixel-wise convolution operation. The binary features generated from (2) are influenced by the illumination variations as the knuckle images were acquired under ambient lighting. The influence of noise from such source is minimized by performing morphological opening (F_b^o, G_b^o) and closing (F_b^c, G_b^c) operations, on the templates generated from (2). These templates are used to consolidate the match scores from the two corresponded local knuckle image regions. The match score s_i between two translated or

the corresponded i^{th} sub-image blocks, between the normalized knuckle image F and G , is computed as follows:

$$s_i = \sum \sum [w_1 \times \text{XOR}(F_b, G_b) + w_2 \times \text{XOR}(F_b^o, G_b^o) + w_3 \times (F_b^c, G_b^c)] \quad (3)$$

where the w_1, w_2 and w_3 represents the weights assigned to the each of the three cases and were empirically fixed as 3, 1, 1, respectively, for all the experimental results reported in this paper. The XOR is the Boolean operator employed to compute the Hamming distance between two binary sub-images. Similarly, the match scores from all the grid points are computed using (3) and averaged to generate the final or the consolidated match score between the two matched finger knuckle images.

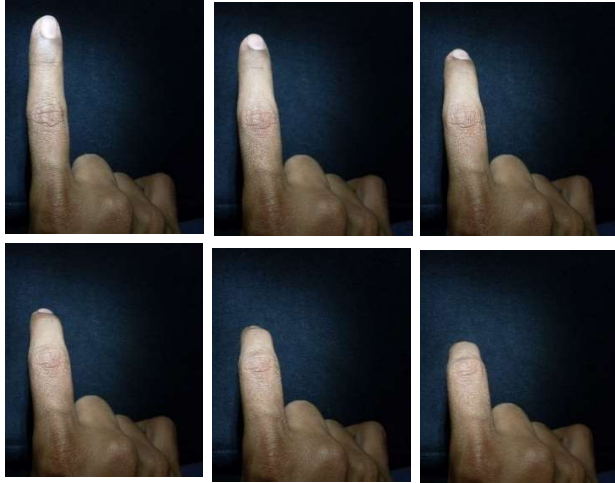


Figure 4: Completely contactless finger knuckle images with severe pose deformations. Each of the subject’s right-hand index finger provides knuckle images under six different poses as shown from the above sample images.

IV. EXPERIMENTS AND RESULTS

This work uses recently introduced PolyU contactless finger knuckle database version 3 [13] in which the finger knuckle images are acquired under different poses. There are a total of six different poses for each of the 221 different subjects index fingers. were acquired from 221 volunteers using different smartphones. The images are acquired using the mobile phone camera and under indoor and outdoor environment which presents more realistic challenges for the real-world applications. All the volunteers were requested to present their index fingers under six different poses, where the first image was acquired while the finger was straight while the last or sixth image representing the image when finger was bent excessively. Such sample images are shown in Figure 4. Please refer of [2] for more details on the data acquisition and the method used to automatically detect the finger knuckle regions. The segmentation images are provided along with this database and were used to ascertain the authentication performance in this work.

Unlike for the earlier methods such as in [5] which require image enhancement, the approach adopted in this work does not use any enhancement of the ROI knuckle images. The match protocols for the two-session (inter-day) and one-session (intra-day) finger knuckle images are exactly same as employed in [2]. The baseline methods have used phase only

correlation [14] and band-limited phase only correlation [3]. Therefore, this approach was also attempted to ascertain the comparative performance. The effectiveness of the phase-based correspondence point estimation for matching severely deformed finger knuckle images is firstly visualized from the location in correspondence points among the deformed knuckle images from the same subject or the finger. Figure 4 presents such image samples that illustrate the location of correspondence or grid points when the first or straight pose knuckle image is matched with other six pose images from the same user but using the second session. The image samples selected in Figure 5-7 are from subject 47 in this database.

The first two image columns, in each of the Figures 5-7, are the original or knuckle ROI images from same subject, the third image shows the grid point for the first image, and the fourth image is the corresponding grid point for the second image after computing the correspondence point locations. The match scores obtained from the two respective images in each row are also presented in the respective Figure captions in the same order. shown are in the same order as the matches. In summary, the first images in Figure 5-7 columns are the same subjects’ images from the second session, where the second images correspond to the six different images in different row from same subject in the first session imaging.

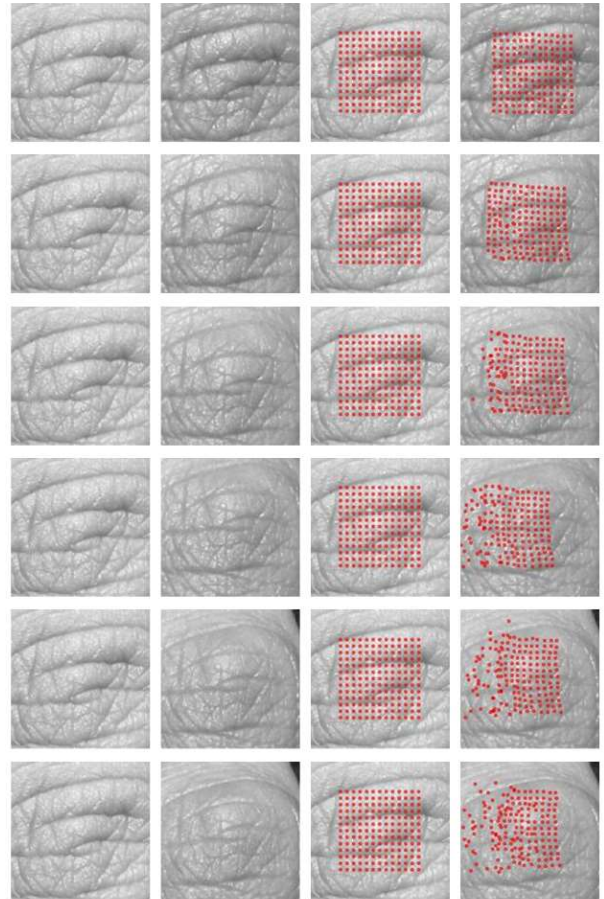


Figure 5: Matching second session *first* image from same subject with different pose knuckle images acquired in the first session. The match scores, respectively for the first-row image pairs to the last row image pairs are 0.445, 0.646, 0.775, 0.921 0.927, and 1.027.

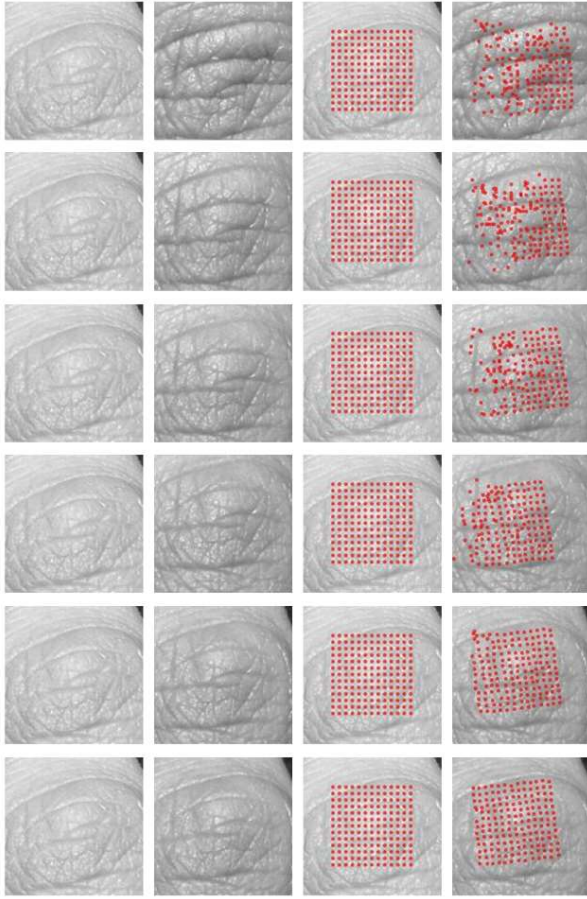


Figure 6: Matching second session *fifth* image from same subject with different pose knuckle images acquired in the first session. The match scores, respectively for the first-row image pairs to the last row image pairs are 1.177, 1.068, 0.956, 0.849, 0.803 and 0.6440.

Table 1: Summary of match score statistics from experiments.

	Two-Session Database	One-Session Database
Number of Genuine Scores	624 (6×104)	1326 (221× 6)
Number of Impostor Scores	64272 (6×104× 103)	145860(6×221×220)/ 2
Range of Genuine Scores	0.4453 to 1.3883	0.4448 to 2.0089
Mean of Genuine Scores	0.9881	1.0260
Range of Impostor Scores	0.5710 to 1.4776	1.5150 to 2.0699
Mean of Impostor Scores	1.3232	1.8570
Equal Error Rate	14.74% (Th=1.2899)	6.03% (Th= 1.7738)

Th: Decision Threshold at Equal Error Rate

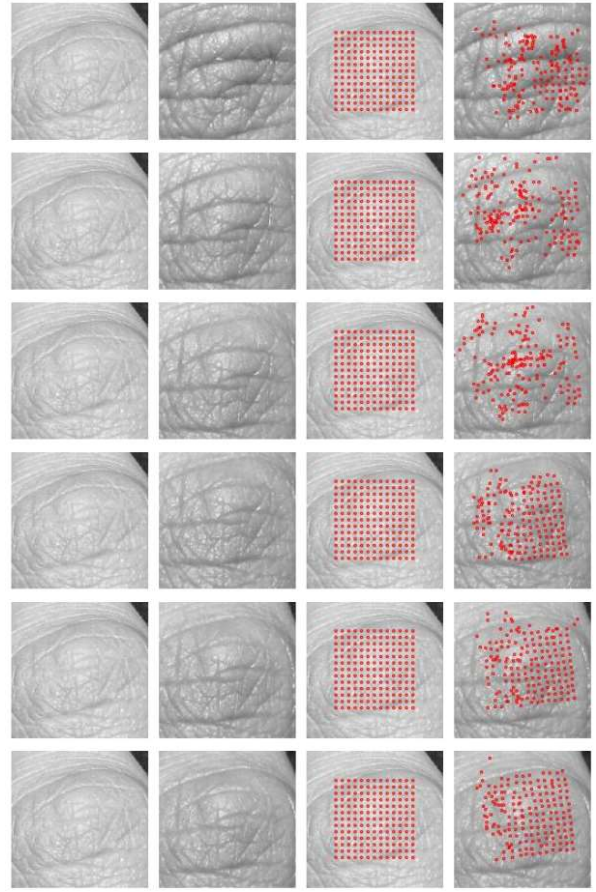
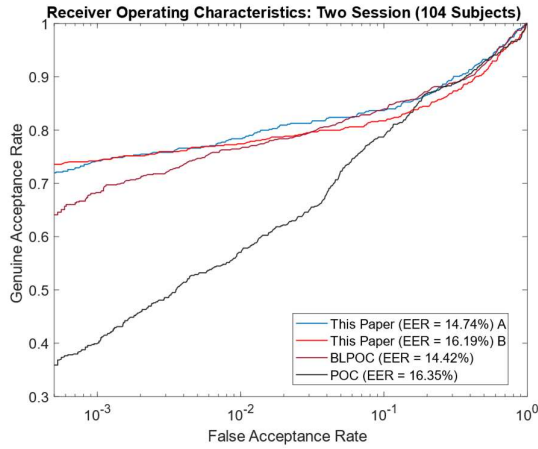


Figure 7: Matching second session *last/sixth* image from same subject with different pose knuckle images acquired in the first session. The match scores, respectively for the first-row image pairs to the last row image pairs are 1.246, 1.256, 1.305, 1.091, 1.069, and 0.973.

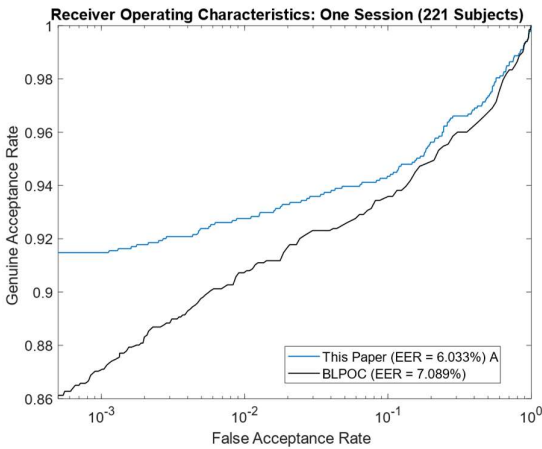
It can be observed from the match scores in Figure 5 that the match score gradually degrades, with worst or the highest when first pose image is matched with the last or severely deformed pose images. However even the worst-case match score in Figure 5 is smaller as compared to the impostor scores (please see Table 1 for exact decision threshold at EER) and therefore these image pairs can be considered as matched.

The receiver operating characteristics (ROC) from the authentication experiments is shown in Figure 8. Table 1 presents number of match scores generated from two different set of experiments and includes other relevant statistics relating to the reproducibility of the experiments. The ROC in Figure 8(a) indicates the results from two potential masks or the spatial filters to encode the features. The results labelled ‘A’ uses the filter shown in Figure 3(a) while the results labelled ‘B’ use the filter shown in Figure 3(b). The results from these two filters are quite similar, with the filter ‘A’ achieving better performance. Therefore, this filter was only used for the single session experiments in Figure 8(b). The results in Figure 8 consistently indicate superior matching performance over the baseline methods using BLPOC and POC. Matching knuckle features using local feature descriptors is also computationally simpler and the methods using POC or BLPOC requires FFT and IFFT operations which are known to be quite complex. The match score and the distribution of correspondence points in Figure 7 images

indicates that even when the when the two images from same subject but with extreme pose changes (last row image pair) can generate low match score or higher similarity confidence. The degradation in match score is severe when the difference in poses between the matched finger knuckle images are large.



(a)



(b)

Figure 8: The ROC for matching (a) two-session contactless finger knuckle images and (b) one session contactless finger knuckle images acquired from 221 different subjects.

V. DISCUSSION

A range of experiments were performed to adopt different feature descriptors, in an attempt to generate best performance for matching deformed finger knuckle images. The method detailed in [2] was also attempted for the authentication problem but the results were quite poor. The comparative roc performance using *ternary* contrast context vector (TCCV) [2], and its combination using spectral domain matching, is presented in Figure 9. These results indicate that correspondence point-based matching considered in this work can offer superior matching performance for the deformed finger knuckle images.

There are a range of other spatial-domain feature descriptors that have shown to offer attractive performance for matching biometric images. Therefore, similar to as in [2], a number of other matchers were attempted to ascertain verification performance for matching deformed knuckle images. The multi local binary (LBP) [22] used three scales to consolidate

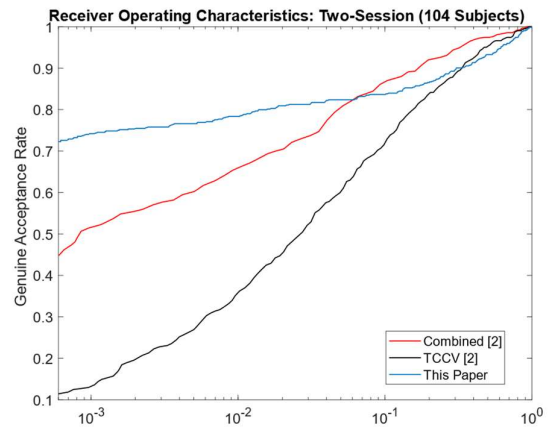
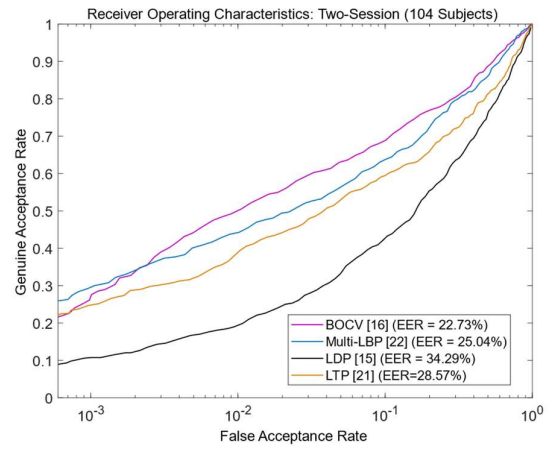
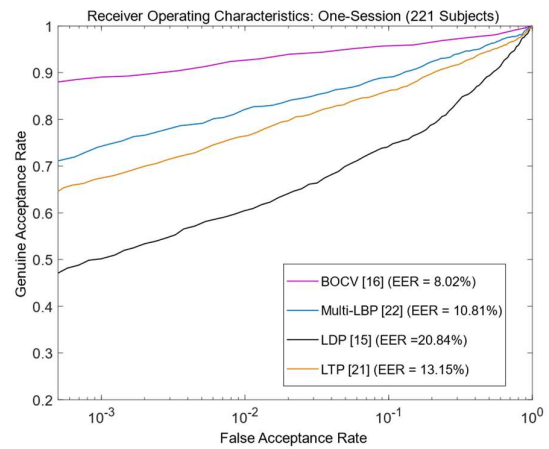


Figure 9: Comparative performance for two-session contactless finger knuckle matching using TCCV [2] for the verification problem considered in this paper.



(a)



(b)

Figure 10: Comparative performance using other feature descriptors for (a) two session and (b) single-session finger knuckle images.

the scores. The binary orientation co-occurrence vector (BOCV) [16] has shown highly accurate results for the palmprint matching and was also attempted. The BOCV matcher used 49×49 size block and thresholds of 0.06 and

0.3. These parameters were empirically selected to achieve the best performance. Two other matchers, *i.e.* local derivative patterns (LDP) [17] and local ternary patterns (LTP) [21], were attempted. The experiments for LDP used 3×3 size blocks with step size of 18. These comparative results for two-session and one-session verification performance are presented in Figure 10. These results indicate that BOCV offers superior performance than other considered methods. However as can be observed from the results in Figure 8, the performance from the approach detailed in section 2 is significantly better and is suggested for matching finger knuckle images with severe pose deformations.

VI. CONCLUSIONS AND FURTHER WORK

Completely contactless finger knuckle identification can offer promising alternative to address hygiene and privacy related concerns with the established biometric modalities. Capabilities to accurately match deformed finger knuckle image pairs is also highly desirable for a range of law enforcement applications, *e.g.* [10]. However, completely contactless finger knuckle acquisition can offer extremely high intra-class variations, largely due to involuntary finger poses or the view-angle changes. Therefore, the knuckle verification problem considered in this paper is highly challenging and not attempted earlier in the best of our knowledge. The results presented in this paper should be considered preliminary, or the first attempt for the user verification using severely deformed finger knuckle images.

The method introduced in [2] to detect the finger knuckle images under varying poses has several limitations. It can be observed from this reference that many of the detected or segmented images fail to represent the true region of interest, *i.e.*, major finger knuckle region. This is another reason for relatively lower performance observed from the verification results presented in this paper. Further work is required to accurately detect such finger knuckle regions and mask-RCNN based detectors [18] have shown to work well under complex backgrounds and is suggested in the further extension of this work. Deep learning-based methods have shown to offer attractive performance for a range of computer vision and biometrics applications. However limited availability of deformed finger knuckle images has posed severe constraints in attempting such methods for the verification tasks. The match accuracy indicated in results in Figure 5-8 is high and attractive for forensic applications but not yet attractive for e-business or other civilian applications. Therefore, further work is required to develop advanced methods that can generate more accurate results to utilize full potential from this biometric modality. This work used more convenient protocol to match second session images, with the *best* of the first session or registration images scores (Table 1, 6×104 or 624 genuine match scores). Further work should consider more challenging protocols where each of the second session images are matched with each of the first session images, *i.e.*, $6 \times 6 \times 104$ or 3744 genuine match scores, to evaluate the effectiveness of the future or proposed algorithms for the surveillance and forensic applications.

REFERENCES

[1] K. Takita, M.A. Muquit, T. Aoki, and T. Higuchi. A sub-pixel correspondence search technique for computer vision applications.

IEICE Trans. Fundamentals, vol. E87-A, no. 8, pp/ 1913-1923, Aug. 2004.

[2] A. Kumar, "Toward pose invariant and completely contactless finger knuckle recognition," *IEEE Trans. Biometrics Behav. Identity Sci.*, vol. 1, no. 3, pp. 201–209, Jul. 2019.

[3] K. Ito, T. Aoki, and S. Iitsuka, "A palmprint recognition algorithm using phase-based correspondence matching," *Proc. Int'l Conf. Image Processing*, pp. 1977-1980, Nov. 2009.

[4] G. Jaswal, A. Kaul, and R. Nath. Knuckle print biometrics and fusion schemes—overview, challenges, and solutions. *ACM Comp. Surv.*, 2016.

[5] A. Kumar and Y. Zhou, "Human identification using knucklecodes," *Proc. 3rd Intl. Conf. Biometrics, Theory and Applications, BTAS'09*, pp. 147-152, Washington DC, USA, Sep. 2009

[6] L. Zhang, L. Zhang, D. Zhang and H. Zhu, "Online finger-knuckle-print verification for personal authentication," *Pattern Recognition*, Jul. 2010.

[7] J. Kim, K. Oh, B. S. Oh, Z. Lin and K. A. Toh, "A line feature extraction method for finger-knuckle-print verification," *Cogn. Comput.*, 2018.

[8] A. Kumar and Z. Xu, "Personal identification using minor knuckle patterns from palm dorsal surface," *IEEE Trans. Info. Forensics & Security*, pp. 2338-2348, Oct. 2016.

[9] Q. Zheng, A. Kumar, and G. Pan "A 3D Feature Descriptor Recovered from a Single 2D Palmprint Image," *IEEE Trans. Pattern Analysis & Machine Intell.*, vol. 38, no. 6, pp. 1272-1279, Jun 2016.

[10] M. Bromley Paedophile Dean Hardy Jailed for 10 Years, *Bromley Times*, Jan. 2012. http://www.bromleytimes.co.uk/news/courtcrime/bromley_paedophile_dean_hardy_jailed_for_10_years_1_1176957.

[11] G. K. O. Michael, T. Connie, and A. B. J. Teoh, "Touch-less palm print biometrics: Novel design and implementation," *Image Vis. Comput.*, 768 vol. 26, no. 12, pp. 1551–1560, 2008.

[12] A. Kumar, "Towards more accurate matching for contactless palmprint images," *IEEE Trans. Info. Forensics & Security*, vol. 14, no.1, pp. 34-47, Jan. 2019.

[13] The Hong Kong Polytechnic University Contactless Finger Knuckle Images Database (Version 3.0), <https://www4.comp.polyu.edu.hk/~csajaykr/fn2.htm>, 2019

[14] K. Ito, T. Aoki, H. Nakajima, K. Kobayashi, T. Higuchi, "A palmprint recognition algorithm using phase-only correlation," *IEICE Trans. FECCS*, vol. E91-A, pp. 1023-1030, April 2008.

[15] B. Zhang, Y. Gao, S. Zhao J. Liu, "Local derivative pattern versus local binary pattern: Face recognition with high-order local pattern descriptor," *IEEE Trans. Image Process.* 19, pp. 533–544, 2010.

[16] Z. Guo, D. Zhang, L. Zhang, W. Guo, "Palmprint verification using binary orientation co-occurrence vector," *Pattern Recogn. Lett.*, vol. 30, pp. 1219–1227, 2009.

[17] A. Kumar and Ch. Ravikanth. Personal authentication using finger knuckle surface. *IEEE Trans. Info. Forensics & Security*, Mar. 2009.

[18] Y. Liu, A. Kumar, "Contactless Palmprint Identification using Deeply Learned Residual Features," *IEEE Trans. Biometrics Behav. Identity Sci.*, vol. 2, no. 2, pp. 172–181, Apr. 2020.

[19] Q. Zheng, A. Kumar, and G. Pan. A 3D Feature Descriptor Recovered from a Single 2D Palmprint Image. *IEEE Trans. Pattern Analysis & Machine Intell.*, vol. 38, no. 6, pp. 1272-1279, Jun 2016.

[20] V. Roux, S. Aoyama, K. Ito, T. Aoki, "Performance improvement of phase-based correspondence matching for palmprint recognition," *Proc. CVPR 2014 Biometrics Workshop*, pp. 77, 2014.

[21] X. Tan and B. Triggs, "Enhanced local texture feature sets for face recognition under difficult lighting conditions," *IEEE Trans. Image Process.*, vol. 19, pp. 1635-1650, Jun. 2010.

[22] T. Ojala, M. Pietikäinen, and T. Mäenpää, "Multiresolution gray-scale and rotation invariant texture classification with local binary patterns," *IEEE Trans. Pattern Anal. Mach. Intell.*, vol. 24, pp. 971-987, 2002.

[23] S. Aoyama, K. Ito, and T. Aoki, "Finger-knuckle-print recognition using BLPOC-based local block matching," *Proc. ACPR*, pp. 525-529, Nov. 2011.